Tiam1 interaction with the PAR complex promotes talin-mediated Rac1 activation during polarized cell migration

Shujie Wang,[1,2] Takashi Watanabe,[1] Kenji Matsuzawa,[1] Akira Katsumi,[3] Mai Kakeno,[1] Toshinori Matsui,[1] Feng Ye,[4] Kazuhide Sato,[1] Kiyoko Murase,[1] Ikuko Sugiyama,[1,5] Kazushi Kimura,[2] Akira Mizoguchi,[2] Mark H. Ginsberg,[4] John G. Collard,[6] and Kozo Kaibuchi[1,5]

[1]Department of Cell Pharmacology, Nagoya University Graduate School of Medicine, 65 Tsurumai, Showa, Nagoya, Aichi 466-8550, Japan
[2]Department of Neural Regeneration and Cell Communication, Mie University Graduate School of Medicine, 2-174 Edobashi, Tsu, Mie 514-8507, Japan
[3]Department of Hematology and Oncology, Nagoya University Graduate School of Medicine, 65 Tsurumai, Showa, Nagoya, Aichi 466-8550, Japan
[4]Department of Medicine, University of California San Diego, La Jolla, CA 92093
[5]Japan Science and Technology Agency (JST), Core Research for Evolutional Science and Technology (CREST), 65 Tsurumai, Showa, Nagoya, Aichi 466-8550, Japan
[6]The Netherlands Cancer Institute, Division of Cell Biology, Plesmanlaan 121, 1066 CX Amsterdam, Netherlands

Migrating cells acquire front-rear polarity with a leading edge and a trailing tail for directional movement. The Rac exchange factor Tiam1 participates in polarized cell migration with the PAR complex of PAR3, PAR6, and atypical protein kinase C. However, it remains largely unknown how Tiam1 is regulated and contributes to the establishment of polarity in migrating cells. We show here that Tiam1 interacts directly with talin, which binds and activates integrins to mediate their signaling. Tiam1 accumulated at adhesions in a manner dependent on talin and the PAR complex. The interactions of talin with Tiam1 and the PAR complex were required for adhesion-induced Rac1 activation, cell spreading, and migration toward integrin substrates. Furthermore, Tiam1 acted with talin to regulate adhesion turnover. Thus, we propose that Tiam1, with the PAR complex, binds to integrins through talin and, together with the PAR complex, thereby regulates Rac1 activity and adhesion turnover for polarized migration.

Introduction

Directional cell migration is essential for various physiological processes such as embryonic development, angiogenesis, wound healing, and tumor invasion (Petrie et al., 2009). In response to extracellular and cell adhesion signals, cells acquire a polarized morphology with a leading edge at their front and a trailing tail at the rear (Ridley et al., 2003). This front-rear polarity is established along the directional axis, with signaling molecules, adhesions, and the cytoskeleton distributed asymmetrically. Among the signaling molecules that control polarity, the Rho family GTPases, including Rac1, Cdc42, and RhoA, play key roles in regulating the cytoskeleton and cell adhesions (Fukata et al., 2003; Jaffe and Hall, 2005). The activities of the Rho family GTPases are controlled by three classes of regulators: guanine nucleotide exchange factors (GEFs), GDP dissociation inhibitors (GDIs), and GTPase-activating proteins (GAPs; Rossman et al., 2005; Bos et al., 2007; Garcia-Mata et al., 2011).

Another major player in cell polarization is the PAR complex, composed of PAR3, PAR6, and atypical protein kinase C (aPKC), which functions in various cell polarization events including apico-basal, neuronal, and front-rear polarity (Suzuki and Ohno, 2006; Goldstein and Macara, 2007; Etienne-Manneville, 2008). The PAR complex cooperates with Rho family members for polarized migration (Iden and Collard, 2008). Activated Cdc42 binds to PAR6, which then associates

S. Wang and T. Watanabe contributed equally to this paper

Correspondence to Kozo Kaibuchi: kaibuchi@med.nagoya-u.ac.jp

Abbreviations used in this paper: aPKC, atypical PKC; DH, Dbl homology; FERM, band 4.1/ezrin/radixin/moesin; FL, full-length; FN, fibronectin; FRET, fluorescence resonance energy transfer; GEF, guanine nucleotide exchange factor; PDZ, PSD-95/Dlg/ZO-1; PH, pleckstrin homology; pY, phosphotyrosine; RBD, Ras-binding domain; TIRFM, total internal reflection fluorescent microscopy.

The Rockefeller University Press $30.00
J. Cell Biol. Vol. 199 No. 2 331–345
www.jcb.org/cgi/doi/10.1083/jcb.201202041

with PAR3 and aPKC, leading to aPKC activation (Suzuki and Ohno, 2006; Goldstein and Macara, 2007). PAR3 interacts with Tiam1, a Rac-specific GEF, and further forms a complex with aPKC, PAR6, and Cdc42, thereby mediating Cdc42-induced Rac1 activation (Nishimura et al., 2005). The PAR–Tiam1 complex participates in front-rear polarity for persistent migration (Pegtel et al., 2007). The RhoA effector Rho-kinase/ROCK/ROK phosphorylates PAR3 and disrupts the PAR complex, resulting in Rac1 inactivation to prevent ectopic protrusion from the rear of the migrating cells (Nakayama et al., 2008).

Asymmetry in the dynamics of adhesions between cells and their surrounding ECM is critical for polarized cell migration (Parsons et al., 2010; Huttenlocher and Horwitz, 2011). The integrins, composed of α and β subunits, act as primary ECM receptors to mediate and control cell–ECM adhesion (Hynes, 2002). The binding of integrins to the ECM activates intracellular signaling pathways that regulate migration (outside-in signaling), whereas the affinity of integrins for the ECM can be regulated by signals within cells (inside-out signaling). Talin is a key participant in both outside-in and inside-out signaling (Critchley, 2009; Moser et al., 2009). Talin associates directly with the cytoplasmic region of integrin β, and increases binding affinities of integrins for the ECM. Furthermore, talin functions as a molecular bridge to link integrins both with the actin cytoskeleton, which enables the cell to exert tensile force on the ECM, and with various signaling molecules (Critchley, 2009; Moser et al., 2009).

Within polarized migrating cells, Rac1 and Cdc42 are activated at the leading edge to generate a vectorial protrusion in the direction of migration (Kraynov et al., 2000; Itoh et al., 2002). Although RhoA controls contractility to restrict protrusions in the cell body, recent biosensor studies indicate that Rho is also activated at the leading edge to initiate protrusive event, and that Rac1 and Cdc42 reinforce and stabilize newly expanded protrusions (Pertz et al., 2006; Machacek et al., 2009). The leading protrusion is stabilized by its adherence to the surrounding ECM through adhesion receptors such as integrins, which in turn activates Rac1 and Cdc42 to further induce small adhesions at the leading edge. Many of these adhesions fail to mature and are instead disassembled, but some mature behind the leading edge through the action of RhoA and myosin. Mature adhesions are eventually disassembled underneath the advancing cell body and at the rear ends of motile cells (Parsons et al., 2010). Rac1 accumulates at adhesions and participates in adhesion turnover, presumably acting through its effector PAK and/or by antagonizing RhoA (ten Klooster et al., 2006; Huveneers and Danen, 2009; Parsons et al., 2010; Guilluy et al., 2011). The positive circuitry between Rac1 and integrins is critical for maintaining the directionality of migrating cells (Ridley et al., 2003; Parsons et al., 2010).

Although several Rac GEFs including Tiam1, DOCK180, and βPIX are implicated in Rac1 activation downstream of integrins (Huveneers and Danen, 2009; Parsons et al., 2010), how integrins activate Rac1 during cell adhesion, polarization, and migration remains elusive. Because the PAR–Tiam1 complex is involved in front-rear polarity (Goldstein and Macara, 2007; Etienne-Manneville, 2008; Iden and Collard, 2008), we here explored the mode of action of Tiam1 in polarized migration.

Results

Talin is a novel Tiam1-interacting protein

To explore the roles of Tiam1 in polarized cell migration, we isolated Tiam1 interactors from a porcine brain cytosol fraction by affinity column chromatography using beads coated with GST (control), GST-Tiam1-PHnCCEx, or GST-Tiam1-PDZ(PSD-95/Dlg/ZO-1)4 (Fig. 1 A). The PHnCCEx fragment comprises the region from the pleckstrin homology (PH) domain to the Ras-binding domain (RBD), whereas PDZ4 contains the RBD, PDZ, and Dbl homology (DH) domains. Silver staining revealed several bands specific to the eluates from the Tiam1-PDZ4 column. Mass spectrometric analysis identified those proteins as talin, spectrin (α-fodrin), and TBP-interacting protein 120 (TIP120; Fig. 1 B). Because talin is an essential cytoskeletal protein that contributes to integrin activation and cell migration (Critchley, 2009; Moser et al., 2009), we hereafter focused on talin. Of note, Tiam1 was also detected in the eluates from the column coated with the N-terminal regions of talin1 (unpublished data). The interaction of Tiam1 with talin was further confirmed by immunoprecipitation. From COS7 cell lysates, HA-fused Tiam1 coprecipitated with EGFP-fused talin1 (Fig. 1 C). From the lysates of cultured cells, talin was also detected in the precipitates of Tiam1, but not in that of control IgG or unrelated protein Ras-GRF (Fig. 1 D), suggesting the specific association between Tiam1 and talin.

Talin binds directly to Tiam1

The band 4.1/ezrin/radixin/moesin (FERM) domain near the N terminus of talin is responsible for integrin binding and activation (Critchley, 2009; Moser et al., 2009). We characterized the interaction of Tiam1 with talin by immunoprecipitating lysates from COS7 cells expressing both Tiam1-HA and myc-tagged talin1 fragments (Fig. 2, A and B). Consistent with affinity column chromatography of talin1, Tiam1-HA coprecipitated with the N-terminal regions (1–433 aa and 102–656 aa) of talin1, but with neither the middle (642–1328 aa) nor the C region (1,304–2,023 aa; Fig. 2 B). The talin FERM domain at the N terminus comprises three subdomains (F1, F2, and F3; Critchley, 2009; Moser et al., 2009), and a pull-down assay showed that the F3 subdomain (305–400 aa) was sufficient to bind to Tiam1, and that the expanded regions encompassing the F3 subdomain facilitated this interaction (Fig. 2 C).

Surface plasmon resonance was used to assess the direct interaction of the two proteins. Purified His-fused talin1 head (1–433 aa) bound to a sensor chip coated with GST-Tiam1-PDZ4 in a dose-dependent manner, with a Kd value of ∼430 nM (Fig. 2 D). Taken together, these data indicate that the central region of Tiam1 binds directly to the F3 subdomain of talin.

Tiam1 accumulates at adhesions with talin

In migrating cells, talin-bound integrins are activated and clustered into adhesions, which serve as the mechanical linkages

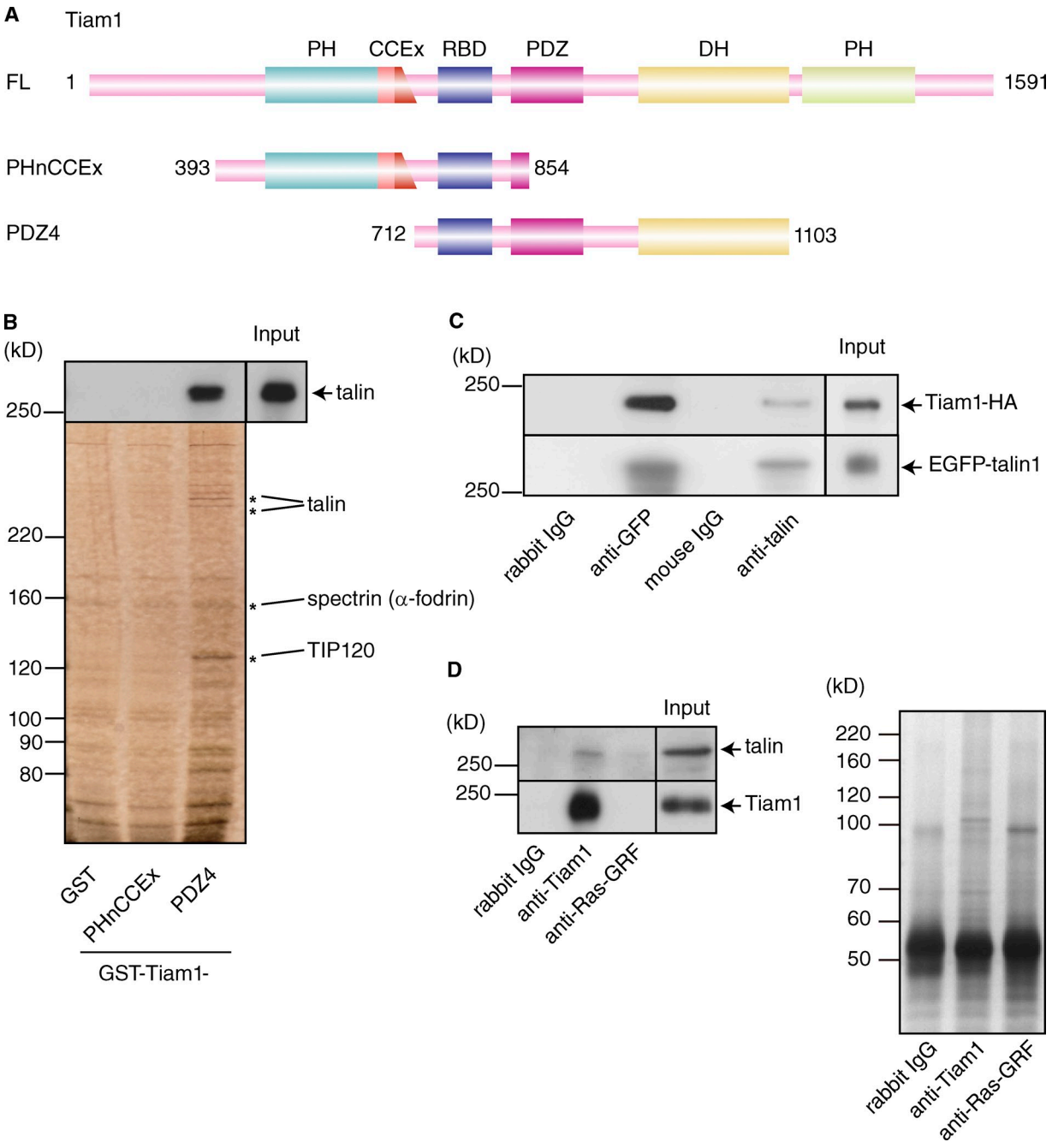

Figure 1. **Talin is a novel Tiam1-interacting protein.** (A) Schematic diagram of Tiam1. The domain organization of Tiam1 and its fragments is represented. (B) The cytoplasmic fraction of a porcine brain homogenate was loaded onto beads coated with GST, GST-Tiam1-PHnCCEX, or GST-Tiam1-PDZ4. Aliquots of the eluate were resolved by SDS-PAGE, followed by silver staining (bottom) or immunoblotting with anti-talin antibody (top). (C) Lysates of COS7 cells expressing both EGFP-talin1 and Tiam1-HA were precipitated with anti-GFP or anti-talin antibody. Tiam1 was coprecipitated with talin by both antibodies. (D) The lysates of U251 cells were precipitated with indicated antibodies, followed by silver staining (right) and immunoblotting (left). Silver staining revealed a specific band pattern in each antibody. Endogenous talin was specifically coprecipitated with Tiam1. Results are representative of more than three experiments.

between the cell and the ECM (mediated in part by talin), and as a platform to concentrate numerous signaling proteins (Zaidel-Bar et al., 2007; Huttenlocher and Horwitz, 2011). To examine the subcellular localization of Tiam1 and talin, we used U251 glioma cells, which express both integrin β1 and β3 that recognize fibronectin (FN; Kawataki et al., 2007), because they acquire a distinct front-rear polarized morphology and migrate persistently on an FN-coated surface (see Fig. 4 D). Cells seeded on FN-coated dishes were immunostained and observed by total internal reflection fluorescence microscopy (TIRFM) to visualize the basal plasma membrane and the immediately proximal cytoplasmic region, i.e., where adhesions are formed. First, we verified our Tiam1 antibody by immunoblot analysis with the cell lysates (Fig. S1, A–C). In migrating U251 cells, talin accumulated at adhesions as expected, whereas Tiam1 appeared as punctate

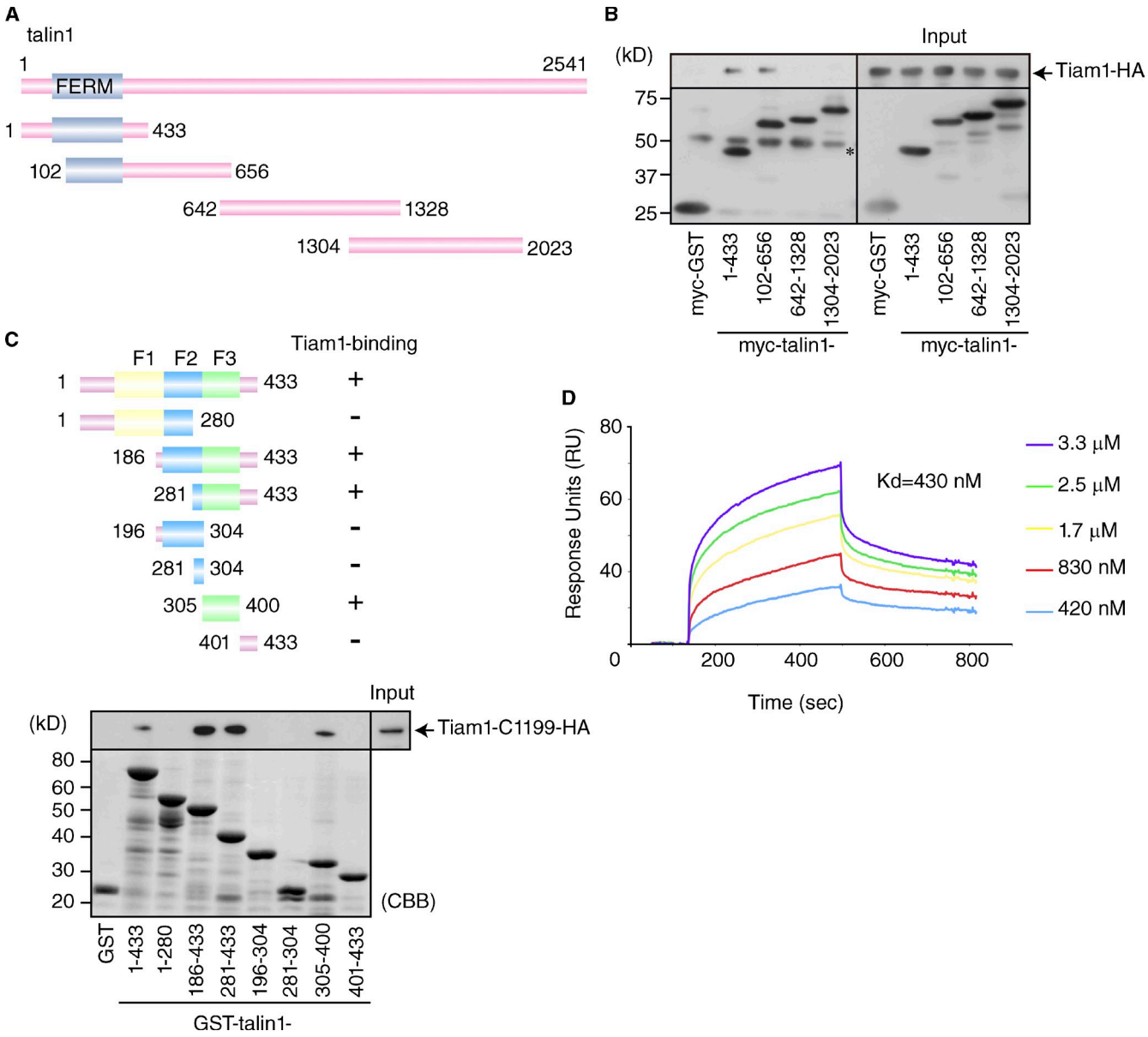

Figure 2. **Talin binds directly to Tiam1.** (A) Schematic diagram of the domain organization of talin1 and its fragments. (B) Lysates of COS7 cells expressing Tiam1-HA and the indicated myc-talin1 fragments were immunoprecipitated with anti-myc antibody. Tiam1 was detected only in the eluates of talin1 1–433 aa and 102–656 aa. Top and bottom panels show immunoblots with anti-HA and anti-myc antibody, respectively. Asterisk indicates immunoglobulin heavy chain. (C) Delineation of the Tiam1-binding region within the talin1 head domain. The fragments used and results are indicated on the top. Tiam1 was most abundant in the eluates of beads coated with talin1 fragments that possessed the F3 subdomain. (D) Sensorgrams of the association and dissociation phases for binding of GST-Tiam1-PDZ4 and His-talin1 1–433 aa. Talin1 (1–433 aa; 0.42–3.3 μM) was injected onto a surface coated with GST-Tiam1-PDZ4. Results are representative of more than three experiments.

staining in an evanescent field that partially colocalized with talin (Fig. 3 A), as well as with other adhesion components such as zyxin and phosphotyrosine (Fig. S1 D). The immunofluorescence of Tiam1 at adhesions was diminished by Tiam1 depletion with siRNA (Fig. 3 C) and absent in Tiam1-deficient MEFs (Fig. S1 E). Tiam1 only localized to a subpopulation of talin-containing adhesions: ∼70% of total talin clusters included Tiam1 (Fig. 3 B; see Materials and methods). Quantitative analysis within the two divided cellular regions, the front (the region facing toward the direction of migration) and the rest, showed that Tiam1 accumulation at adhesions was slightly greater in the front region than in the rest. Tiam1 immunofluorescence was subtly biased toward larger adhesions, whereas no preferential colocalization was observed between phosphotyrosine and talin in the size and the location (Fig. 3 B). We further examined Tiam1–talin colocalization at adhesions by Rho-kinase inhibition, because Rho-kinase is required for the formation and maintenance of tensile adhesions (Parsons et al., 2010). Treatment with Y27632 induced the formation of nascent adhesions, and impaired Tiam1 accumulation (Fig. S1 F). In addition, the short exposure to blebbistatin (20 μM for 5 min) also attenuated Tiam1 accumulation at adhesions (Fig. S1 G). These results indicate that Tiam1 is primarily recruited to talin-containing large tensile

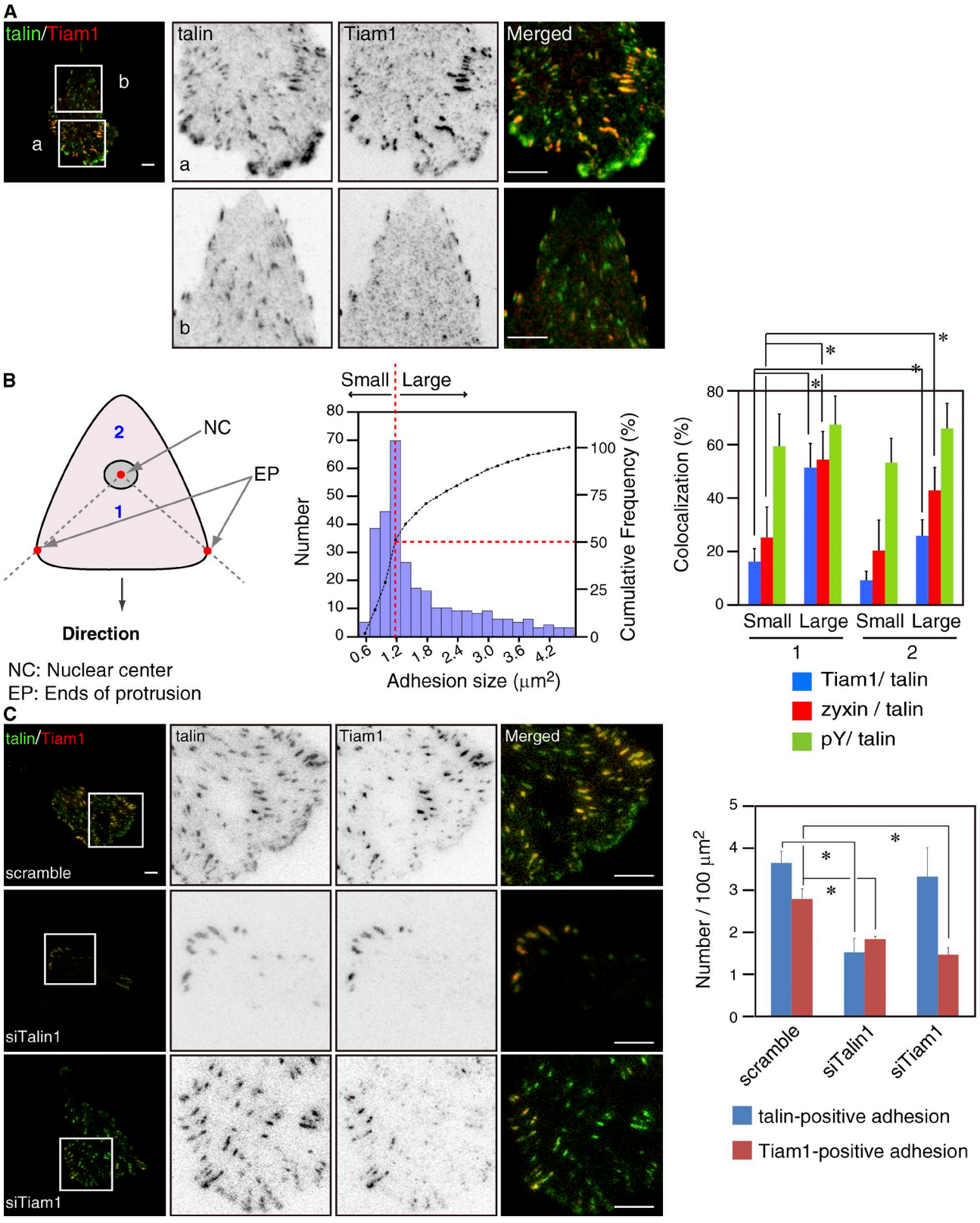

Figure 3. **Tiam1 accumulates at adhesions with talin.** (A) Migrating U251 cells were stained with talin (green) and Tiam1 (red). The images were taken under TIRFM. Insets (a, front region; b, rest) in the left panel are magnified in the right panels. Bars, 10 μm. (B) Size distribution of adhesions and quantification of Tiam1/talin colocalization in migrating U251 cells. Each migrating cell is divided into two regions as indicated diagramatically on the left: front region (1) and rest (2). Small and large adhesions were defined by the distribution of adhesion sizes (histogram, middle). (C) U251 cells transfected with siRNAs indicated in the leftmost images were stained with talin and Tiam1 antibodies. Insets in the leftmost images (merged) are magnified in the panels to the right. Bars, 10 μm. Bar graph on right represents the number of talin- or Tiam1-containing adhesion per 100 μm^2. Data represent the means ± SD of five independent experiments. $n > 50$. *, $P < 0.05$ versus respective control (Tukey's HSD). Results are representative of more than three experiments.

adhesions in U251 cells. Moreover, the FRET analysis of Rac1 in U251 cells showed that the region of higher Rac1 activation sometimes, but not always, overlapped with large adhesions (Fig. S1 H), suggesting that Tiam1 at large adhesion activates Rac1 to control adhesion dynamics for cell migration (see following paragraph).

We next exploited RNAi to address the role of interactions between Tiam1 and talin in the localization of the former. Two siRNAs targeting either Tiam1 or talin1 were prepared and their effectiveness was confirmed by immunoblot analysis (Fig. S2 A). Under the same conditions, we examined the effects of talin1 depletion on Tiam1 and vice versa. Talin1 depletion decreased and delocalized Tiam1 immunofluorescence from adhesions compared with control (Fig. 3 C). When Tiam1 expression was depleted, the appearance of talin was not significantly affected (Fig. 3 C). Thus, we concluded that Tiam1 localizes to adhesions in a manner dependent on its binding to talin (see following paragraph). Of note, because the talin1-depleted cells still expressed talin2 (Fig. S2 B), talin2 and residual talin1 probably account for the talin immunofluorescence and adhesion formation in the talin1-depleted cells. Indeed, when U251 cells were transfected with siRNAs for both talins, adhesions were almost completely absent during the initial phase after adherence to FN (Fig. S2 C), consistent with the previous report (Zhang et al., 2008). In addition, we found that Tiam1 also binds to talin2 in a lower affinity than to talin1 (Fig. S2 D).

Tiam1 and talin are required for adhesion-induced Rac1 activation and cell spreading

Integrin engagement with ECM components such as FN initiates cell adhesion and spreading, which reflect in part Rac1 activation (Price et al., 1998; del Pozo et al., 2000). We examined the involvement of Tiam1 and talin in adhesion-induced Rac1 activation and cell spreading. When suspended U251 cells were plated on a surface coated with FN, the cells underwent spreading (Fig. 4 D). After adhesion, Rac1 activation reached a maximum level after 10 min and then declined to basal level (Fig. 4 A). In the Tiam1- or talin1-depleted cells, this transient Rac1 activation was attenuated (Fig. 4 A). The depletion of talin1 severely abrogated Rac1 activation, whereas that of Tiam1 reduced it to about a half of the level displayed by control cells (Fig. 4 B). Simultaneous depletion of both proteins had no additive effects (unpublished data). Either talin1 or Tiam1 depletion reduced the Rac1 activation before seeding, suggesting that a talin–Tiam1 complex contributes to the basal Rac1 activity. We observed Tiam1 accumulation at a population of adhesions at 30 min after seeding (30 min is a time-point consistent with Rac1 activation; Fig. 4 C). The inhibitory effects of either Tiam1 or talin1 depletion were also observed in different types of cells including Vero fibroblasts and HeLa epithelial cells (unpublished data). When the involvement of other GEFs was examined, depletion of Vav2, mainly expressed in U251 cells among the three Vav isoforms (unpublished data), attenuated Rac1 activation, but to a slightly lesser extent than Tiam1 depletion. Knockdown of DOCK180 or α/βPIX had no apparent effect on Rac1 activation (Fig. S3). These results suggest that Vav2 is also involved in Rac1 activation downstream of integrin to some degree in U251 cells. In addition to U251 cells, when we used another glioma LN229 cells that express DOCK180 at a higher level than U251 cells for Rac1 activation (Jarzynka et al., 2007), either DOCK180 or Tiam1 depletion attenuated adhesion-induced Rac1 activation to a similar degree (unpublished data). This result indicates that Tiam1 is one of the key regulators mediating Rac1 activation at adhesions and that the different requirement of Rac GEF depends on cell type.

When control cells transfected with scramble siRNA were seeded on FN, they developed lamellipodia around the cell periphery, their area and perimeter progressively increased (cell spreading), and they finally acquired a distinct front-rear polarized morphology (Fig. 4, D and E). However, in cells where either Tiam1 or talin1 expression was depleted, lamellipodium development was delayed and, even 4 h after adhesion neither cell spreading nor morphological polarization reached the extent seen in control cells (Fig. 4 D). Concomitantly with the decreased Rac1 activity in either talin1- or Tiam1-depleted cells, their cellular area and perimeter were significantly smaller than control cells, although the progression of cell spreading extended the differences (Fig. 4 E). Taken together with a previous report that Rac1 activation at adhesions generates new membrane protrusion (Xia et al., 2008), our results indicate that the linkage of talin with Tiam1 contributes to membrane expansion during cell spreading. Prominent differences at the later phase are possibly caused by combined deficiencies in integrin-mediated Rac1 activation and linkage of adhesion to actin cytoskeleton, as the previous report proposed (Zhang et al., 2008). Talin1 depletion impaired adhesion-induced Rac1 activation and cell spreading more severely than did Tiam1 depletion. Repeating these experiments with a distinct set of siRNAs yielded similar results (unpublished data). We also found that expression of βPIX could not rescue the deficiencies in Rac1 activation and cell spreading caused by Tiam1 depletion (unpublished data). Of note, the relatively weak phenotypes in our knockdown experiments could be explained by the talin1-specific depletion and involvements of other GEFs (see previous paragraph). Taken together, these observations indicate that both Tiam1 and talin mediate and are required for the propagation of outside-in signals from integrins to activate Rac1.

Tiam1 and talin together control adhesion turnover for polarized cell migration

Migrating cells continuously form and disassemble their adhesions at the leading edge in a process termed adhesion turnover (Parsons et al., 2010). Rac1 accumulates at adhesions and participates in adhesion turnover (Nayal et al., 2006; ten Klooster et al., 2006). The accumulation of Tiam1 at adhesions led us to hypothesize that Tiam1, in conjunction with talin, controls adhesion turnover for polarized cell migration. We monitored adhesion dynamics with EGFP-tagged paxillin in migrating U251 cells. In control cells, adhesions containing EGFP-paxillin formed near the cell edges protruding in the migratory direction; most of them disassembled, but a few

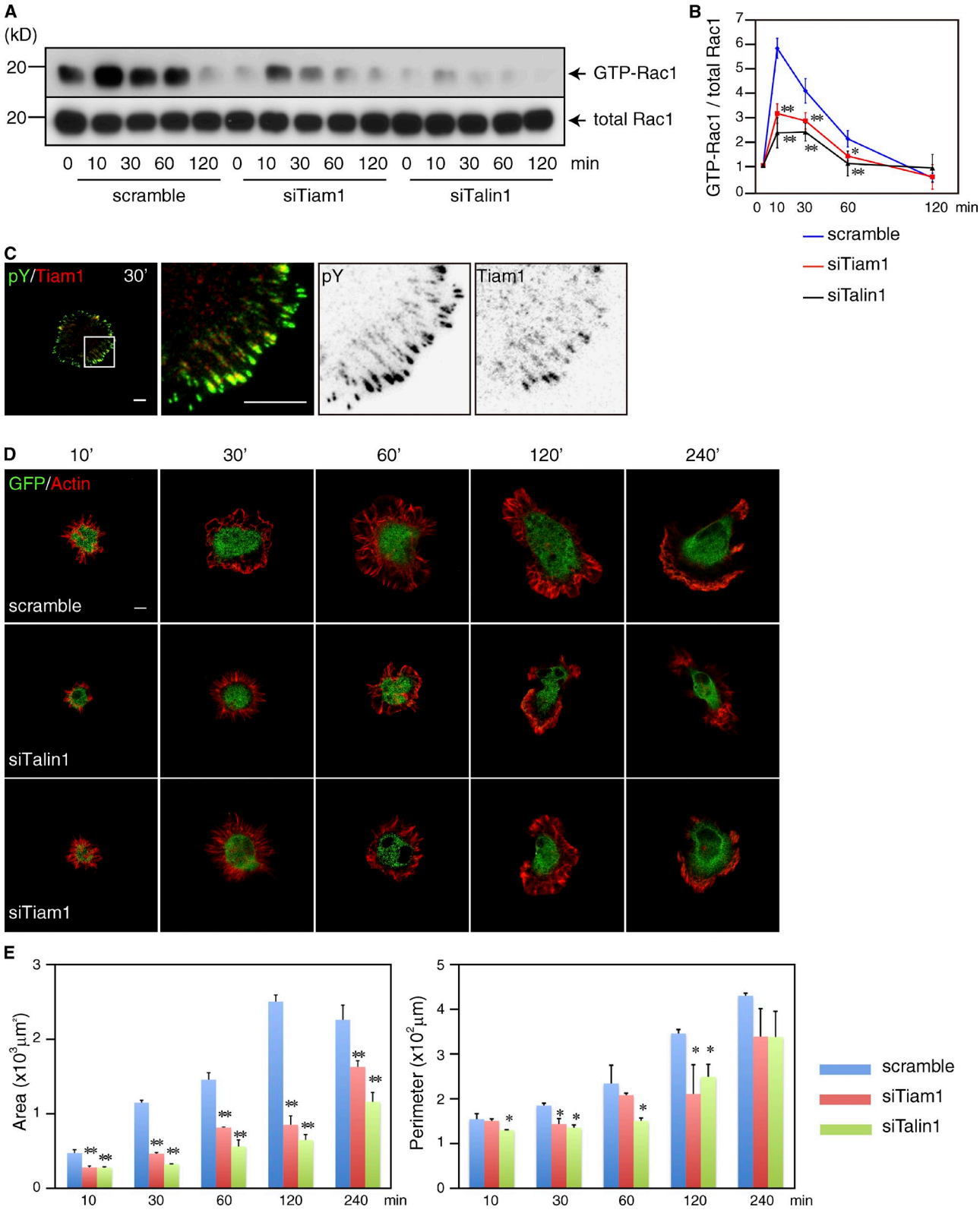

Figure 4. **Tiam1 and talin are required for adhesion-induced Rac1 activation and cell spreading.** (A) U251 cells transfected with the indicated siRNAs were seeded onto FN under serum-free conditions. Rac1 activity was measured by pull-down with PAK-CRIB. Depletion of either talin or Tiam1 impaired transient Rac1 activation upon adhesion. (B) Plots of the quantified data from A. (C) Non-transfected U251 cells were stained at 30 min after seeding with anti-phosphotyrosine (pY) and anti-Tiam1 antibodies. Bars, 10 µm. (D) Images of Tiam1- or talin1-depleted cell spreading on FN. The cells were stained with anti-GFP antibody (green) and phalloidin (red). Bar, 10 µm. (E) Quantification of spreading area and perimeter length during spreading of U251 cells. Results are representative of at least four experiments. Data represent the means ± SD of three independent experiments. $n > 100$. *, $P < 0.05$; **, $P < 0.01$ versus control cells in each time point (B, Student's t test; E, Tukey's HSD).

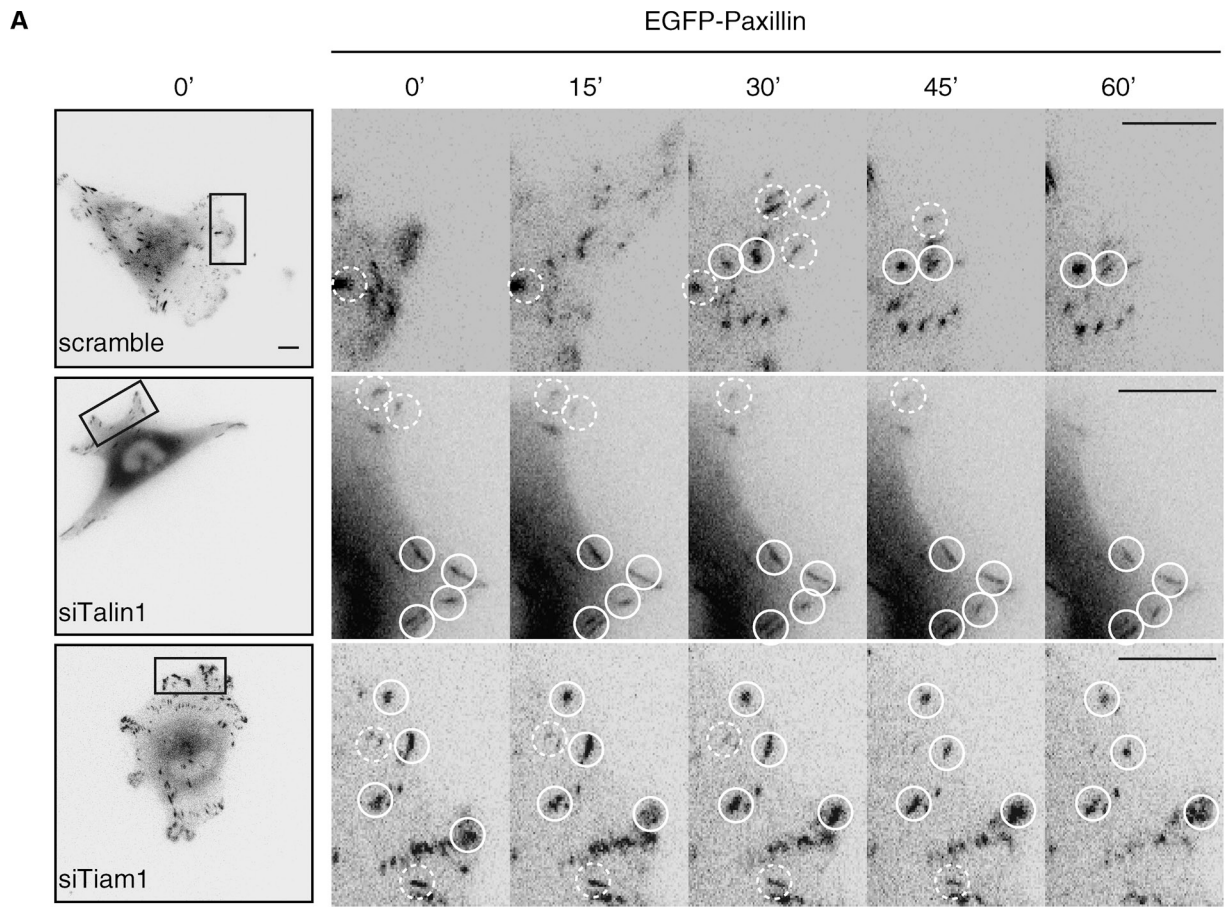

B

Apparent rate constant for assembly (min^{-1})	
scramble	(2.3 ± 0.39) x 10^{-2}
siTalin1	(0.40 ± 0.08) x10^{-2}
siTiam1	(0.34 ± 0.04) x10^{-2}
talin1-WT + siTalin1	(5.5 ± 0.42) x10^{-2}
talin1-A366/368 + siTalin1	(0.61 ± 0.25) x10^{-2}
Rac1-F28L + siTalin1	(2.7± 0.25) x10^{-2}

Rate constant for disassembly (min^{-1})	
scramble	(3.4 ± 0.46) x 10^{-2}
siTalin1	(0.48 ± 0.11) x10^{-2}
siTiam1	(0.78 ± 0.13) x10^{-2}
talin1-WT + siTalin1	(5.8 ± 0.42) x10^{-2}
talin1-A366/368 + siTalin1	(0.70 ± 0.43) x10^{-2}
Rac1-F28L + siTalin1	(2.6± 0.31) x10^{-2}

Figure 5. **Tiam1 and talin together control adhesion turnover for polarized cell migration.** (A) U251 cells were transfected with the indicated siRNAs and EGFP-paxillin. 18 h after seeding onto FN, EGFP-paxillin dynamics was monitored at 5-min intervals for 5 h. Broken and white circles indicate dynamic and static adhesions, respectively. Bars, 10 µm. (B) Apparent rate constants for assembly (left) and rate constant for disassembly (right). Results are representative of more than three independent experiments.

persisted and grew larger behind the protrusions (Fig. 5 A and Video 1). Their apparent rate constant for assembly and rate constant for disassembly were $\sim 2.3 \times 10^{-2}$ and 3.4×10^{-2} min^{-1}, respectively (Fig. 5 B). In the Tiam1- or talin1-depleted cells, assembly and disassembly of adhesions were significantly affected: adhesions assembled slowly, appeared relatively static, and remained for a longer period than those in control cells (Fig. 5 A; and Videos 2 and 3). Indeed, their rates for assembly and disassembly were approximately one-sixth those of control cells (Fig. 5 B). Consistent with the crucial functions of talin at adhesions (Critchley, 2009; Moser et al., 2009), talin1 depletion impaired adhesion dynamics more severely than Tiam1 depletion.

Cell spreading requires the interaction of talin with both Tiam1 and integrin

To address the physiological function of the Tiam1–talin interaction described in the previous paragraph, we first attempted to generate a talin1 mutant that associates with neither Tiam1 nor integrin. Our initial interaction assay suggested that Tiam1 utilizes its PDZ domain as the interface to form a complex with talin1 (Figs. 1 and 2). Based on the previous study suggesting that internal PDZ-binding pseudosequences show a similarity to the C-terminal motifs (Hillier et al., 1999), we screened for a PDZ-binding motif within the F3 subdomain of talin1 and identified and characterized three candidates (366–368, 422–424, and 429–431 aa of talin1). In this way, we found that mutating

talin1 amino acid residues 366 and 368 to alanines (A366/368) decreased its association with Tiam1 by ∼90% relative to wild type (Fig. 6 A). Among previously reported talin1 mutants defective in integrin binding (A358, A359, and A396; García-Mata et al., 2006), A358 and A396 were able to interact with Tiam1, but A359 was not (Fig. 6 A). Reciprocally, the mutant A366/368 bound to integrin β3 to a similar extent to wild-type talin1 under conditions in which A358 binding to integrin, as previously shown, was compromised (Fig. 6 B).

We then studied the effects of these mutants on Tiam1 accumulation at adhesions. The suppression of talin1 expression diminished Tiam1 immunofluorescence at adhesions (Figs. 3 C and 6 C). Transient expression of wild-type talin1 restored Tiam1 localization at adhesions, but neither talin1 mutant A358 nor A366/368 did so (Fig. 6 C). Remarkably, A366/368 localized normally to adhesions, but failed to recruit Tiam1 there. In contrast, A358 was barely detected at adhesions (Fig. 6 C). The similar results were obtained in Vero and HeLa cells (unpublished data). These results strongly support our conclusion that the accumulation of Tiam1 at adhesions depends on its association with talin. Consistent with the idea that Tiam1 and talin together control adhesion dynamics, the expression of wild-type talin1 restored adhesion turnover to control levels, but A366/368 failed to rescue turnover (Fig. 5 B). Furthermore, we found that expression of wild-type talin1 rescued the deficiency in Rac1 activation caused by talin1 depletion, but that of the talin1 mutants failed (Fig. 6 D).

The effects of these mutants on cell spreading were also tested. The expression of wild-type talin1 restored spreading to a level comparable to control (Fig. 6 E); however, reflecting their effects on Tiam1 localization, both talin1 mutants failed to overcome the inhibitory effect of talin1 depletion (Fig. 6 E). The haptotactic cell migration with the Boyden chamber also required the association of talin with both Tiam1 and integrin (Fig. S4). Expression of constitutively active Rac1 (F28L), localized to both the plasma membrane and adhesions (unpublished data), rescued adhesion turnover, cell spreading, and cell migration under the condition in which Rac1 activation responding to integrin engagements was impaired (Figs. 5 B, 6 E, and S4). Taken together, these results indicate that the association of talin with both Tiam1 and integrin is required for the accumulation of Tiam1 at adhesions, adhesion-induced Rac1 activation, adhesion turnover, cell spreading, and cell migration. However, we could not completely exclude the involvement of molecules other than Tiam1.

The PAR complex is involved in Tiam1 targeting to adhesions and in signaling from integrin

Association of Tiam1 with the PAR complex is prerequisite for the activation of Tiam1 during the establishment of front-rear polarity in several migratory cell lines (Pegtel et al., 2007; Nakayama et al., 2008). This prompted us to investigate the involvement of the PAR complex in outside-in signaling from integrin. We first examined the effects of pharmacological inhibition of aPKC on Tiam1 accumulation at adhesions. Cells treated with aPKC inhibitor, a membrane-permeable pseudosubstrate, showed partially impaired Tiam1 accumulation at interior adhesions without affecting talin (Fig. 7 A). Consistently, aPKC directly phosphorylated Tiam1 at the N-terminal region (Fig. S5, A and B). Overexpression of an aPKCλ kinase-dead mutant also abrogated Tiam1 localization, but had negligible effects on talin. On the other hand, overexpression of wild-type aPKCλ enlarged adhesions at the cell margin at which both talin and Tiam1 accumulated (Fig. S5, C and D). When the expression of PAR3, PAR6, or aPKC (both ζ and λ) was suppressed, accumulation of both Tiam1 and talin was negligible at adhesions in the interior region (Fig. 7 B). No statistically significant effects were detectable in the peripheral region. Expression of wild-type PAR3 restored the accumulation of Tiam1 and talin at adhesions in the interior region, but expression of PAR3-Δ4N/1 (lacking the Tiam1-binding region; Nishimura et al., 2005) failed to do so (Fig. 7 C). Of note, PAR3 staining usually, but not always, showed accumulation at interior adhesions, but PAR6 did not (Fig. S5 E), as we reported previously (Itoh et al., 2010). This biased accumulation of PAR3 could account for how the PAR complex differentiates between peripheral and interior adhesions.

We further explored the interplay of the PAR complex with adhesion-mediated signaling and cell spreading. Transfections with siRNAs targeting components of the PAR complex suppressed transient Rac1 activation conspicuously at 30 min after adhesion (Fig. 7 D). Furthermore, during spreading of the PAR complex–depleted cells, the expansion of cell area was suppressed to approximately half the level displayed by control cells (Fig. 7 E). Reminiscent of the effects on Tiam1 localization, introduction of wild-type PAR3 rescued the inhibitory effects of PAR3 depletion nearly to control level, whereas Δ4N/1 expression did not (Fig. 7 E). We also measured Rac1 activation in the PAR3-depleted background, and found that the Tiam1-binding region of PAR3 was required for rescue effects on Rac1 activation (Fig. S5 F), indicating that PAR3 participates in Rac1 activation acting through Tiam1. Together, these results suggest that the PAR complex is necessary for the propagation of outside-in signals from integrin, and that a direct interaction of PAR3 with Tiam1 contributes to the formation of Tiam1-containing adhesions and cell spreading.

Discussion

Interplay between the PAR complex and Rac exchange factor Tiam1 appears to control a variety of polarization processes including those in cell migration. We here demonstrate that Tiam1 localizes to a subpopulation of adhesions, larger adhesions in the front of migrating cells, in a talin-dependent manner. The PAR complex plays critical roles in this biased recruitment of Tiam1. The PAR complex is activated downstream of integrin through Cdc42 and its effector PAR6 at the front of migrating cells (Etienne-Manneville and Hall, 2001). We have shown previously that Tiam1 binds directly to PAR3 and mediates Cdc42-induced Rac1 activation for cell polarity (Nishimura et al., 2005), and that PAR3 partially localizes to interior adhesions (Itoh et al., 2010). We demonstrated previously that PAR3

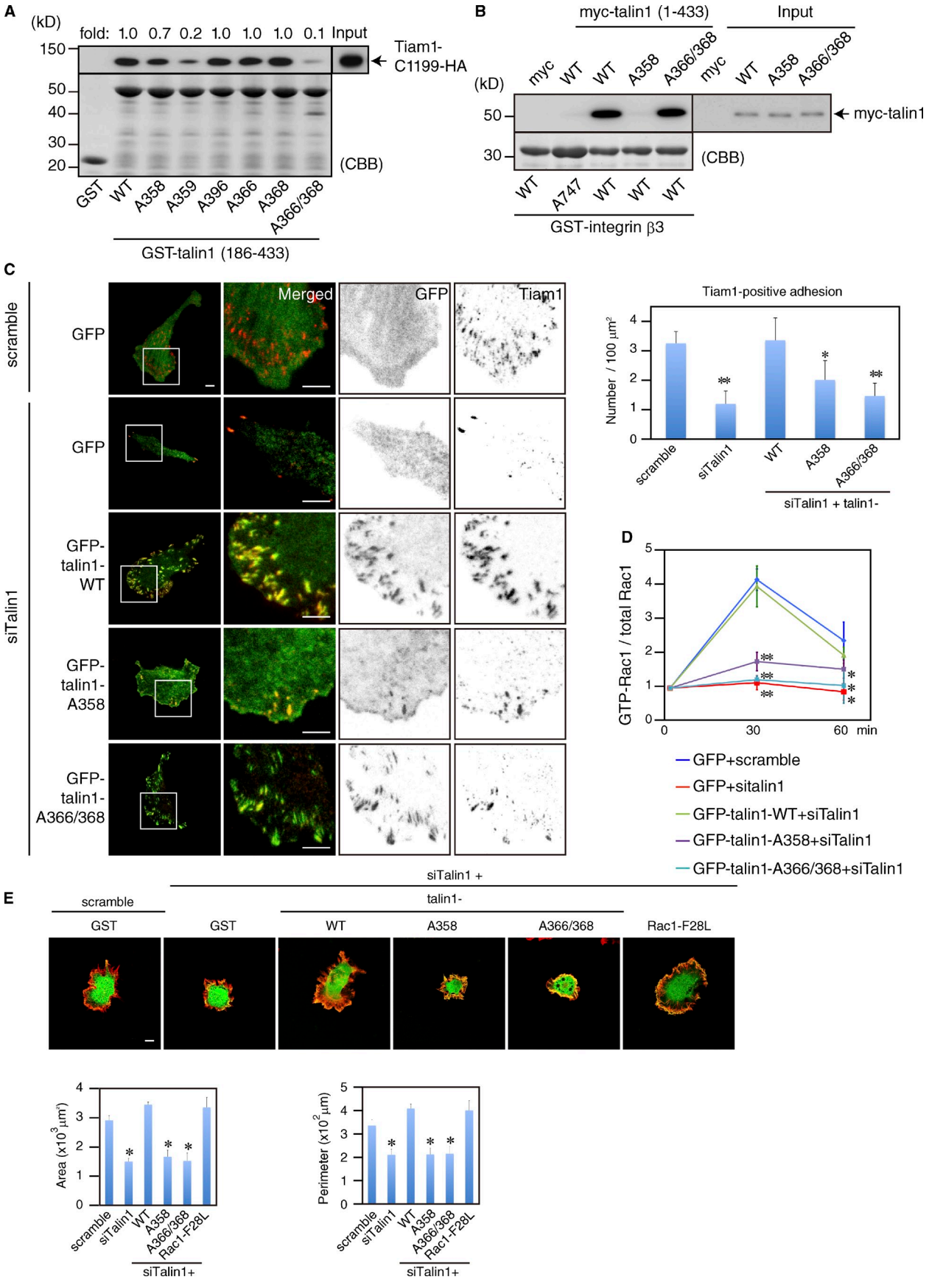

associates with Numb and induces aPKC-mediated Numb phosphorylation, thereby regulating Numb activity (Nishimura and Kaibuchi, 2007). Analogously, we speculate that PAR3 at interior adhesions functions as the scaffold to facilitate Tiam1 phosphorylation by aPKC, which results in a conformational change in Tiam1 that increases its accessibility to talin. Talin then binds and recruits Tiam1, thereby leading to the maintenance of adhesions. Of note, the PAR complex is not absolutely required for Tiam1 recruitment to peripheral adhesions. It is tempting to speculate that the PAR complex primarily controls preferential localization of Tiam1 to interior adhesions. Other Tiam1-binding molecules such as phosphoinositide and Rap1, known for their critical roles at adhesions (Critchley, 2009; Moser et al., 2009; Kim et al., 2011), may be sufficient to localize Tiam1 to peripheral adhesions.

It is widely accepted from biochemical evidence that Rac1 can be activated by integrin engagement with the ECM (Price et al., 1998; del Pozo et al., 2000). A recent study using micropatterning and FRET revealed rapid and localized Rac1 activation at adhesions upon interaction of a motile cell with the ECM (Xia et al., 2008). Our results show that an interactive linkage between integrin, talin, and Tiam1 is likely to be one of the critical regulators for Rac1 activation in response to integrin engagement. We should note that our present study does not contradict the previous studies showing the involvements of other Rac GEFs such as Vav and DOCK180 in adhesion-induced Rac1 activation. The different requirement of Rac GEFs may depend on cell type.

What is the role of Tiam1 at adhesions? We demonstrated that Tiam1 and talin together regulate the adhesion dynamics of motile cells. The effects of talin depletion were overcome by constitutively active Rac1 or wild-type talin, but not by talin mutants defective in binding to either integrin or Tiam1, indicating that complex formation by talin with integrin and Tiam1 is required for adhesion turnover, and that Rac1 controls this turnover downstream of talin and Tiam1. Although we cannot exclude the possibility that activated Rac1 mutant rescues the deficiencies in adhesion turnover and cell migration in a non-adhesion-localized manner, the constitutively active Rac1 mutant appears to rescue the deficiencies at adhesions because it localizes to both the plasma membrane and adhesions. Previous work demonstrated that Rac1 activation regulates adhesion dynamics by forming a positive feed back loop with GIT and αPIX, and Rac1 effector PAK (Nayal et al., 2006). Consistently, we found that pharmacological inhibition of PAK impaired adhesion turnover; both assembly and disassembly of adhesions were attenuated. Concordant with our observations, a recent study has shown that STEF participates in microtubule-dependent Rac1 activation and adhesion disassembly (Rooney et al., 2010). Although the modes of action of those effectors are beyond the scope of this study, these observations indicate that Tiam1 controls adhesion dynamics by acting through Rac1 and its effectors or participating above signaling loop, thereby contributing, with the PAR complex, to polarized migration.

Materials and methods

Plasmids and chemical reagents

We subcloned cDNA fragments of mouse Tiam1 or mouse talin1 into pGEX (GE Healthcare), pEGFP vector (Takara Bio Inc.), pRSET-C1, or pCAGGS-myc. pEGFP-mouse talin1 full-length and several GST-fused chicken talin1 fragments (used in Fig. 2 C) were provided by A. Huttenlocher (University of Wisconsin-Madison, Madison, WI) and D. Critchley (University of Leicester, Leicester, England, UK), respectively. GST-tagged integrin β3 cytoplasmic region was provided by R. Fässler (Max Planck Institute of Biochemistry, Martinsried, Germany). siRNAs were obtained from Greiner Bio-One. The following siRNA sequences were used: control scramble, 5′-CAGUCGCGUUUGCGACUGG-3′; siTalin1-a, 5′-GAUCAUGGUGGAUGACUCU-3′; siTalin1-b, 5′-GAAAUUGCACACAGAUGAU-3′; siTiam1-a, 5′-GCGAAGGAGCAGGUUUUCU-3′; siTiam1-b, 5′-GAACAUUUAACAAGCAACG-3′; siPAR3-a, 5′-GUGAAAUUGAGGUCACGCC-3′; siPAR3-b, 5′-GGCAUGGAGACCUUGGAAG-3′; siPAR6A, 5′-GAGUCGCAUUCGAGGAGAUUU-3′; siPAR6B, 5′-UGGAGACUUACUACCUAUAUU-3′; siaPKCζ, 5′-AGAGGAUCGACCAGUCAGA-3′; siaPKCλ, 5′-CGAACAGCUCUUCACCAUG-3′; siTalin2-a, 5′-CAAUCCUGGUCUCAGCCAAUU-3′; siTalin2-b, 5′-GCUGUUAGCUGCCAAGUCUUU-3′; siαPIX-a, 5′-GAGUUUAAGUUGUCUACGAUU-3′; siαPIX-b, 5′-CAAAGUAGGAGGUUGUCUAUU-3′; siβPIX-a, 5′-CAAAGGAUUUGAUACGACUUU-3′; siβPIX-b, 5′-CUGAUUCAGUGUGCCGGAAUU-3′; siVav2-a, 5′-GUUUGAGAUGGCCAUGUCAUU-3′; siVav2-b, 5′-CGUUUGACAAGACCACCAAUU-3′; siDOCK180-a, 5′-GAAUUAACUAGCACGAUUAUU-3′; and siDOCK180-b, 5′-GACAAUGAAUUUGCGAAUAUU-3′. For the depletion of PAR6 and aPKC, we used a mixture of appropriate siRNAs. For the rescue experiments, we used siRNA-insensitive talin1 or Tiam1 mutants generated with a site-directed mutagenesis kit (Agilent Technologies) by introducing silent mutations within the siRNA target sequence. Talin alanine mutations were also generated in the same way. siRNA-insensitive PAR3 harboring the mutations in siRNA-target sequence and PAR3 mutant lacking the Tiam1-binding region were described previously (Nishimura et al., 2005). Fibronectin and fibronectin-coated dishes were purchased from BD. Antibodies used were as follows: anti-talin (8d4; Sigma-Aldrich), anti-Tiam1 (C16; Santa Cruz Biotechnology, Inc.), anti-Tiam1 raised against DH-PH (Habets et al., 1994), anti-GFP (Roche), anti-GST (Sigma-Aldrich), anti-HA (12CA5), anti-myc (9E10), anti-Rac1 (EMD Millipore), anti-moesin (Kawano et al., 1999), anti-zyxin (Novus Biologicals), anti-phosphotyrosine, anti-Vav2, anti-DOCK180, anti-αPIX, and anti-βPIX (Cell Signaling Technology), and anti-paxillin (BD). Anti-Tiam1 DHPH antibody was characterized with the cell lysates as shown in Fig. S1. Anti-talin2 antibody was provided by D. Critchley and S. Monkley (University of Leicester). We refer to talin1 and talin2 as "talin" when we used an anti-talin antibody (8d4) that recognizes both talin1 and talin2 (Zhang et al., 2008). Anti-PAR3 antibody was provided by S. Ohno (Yokohama City University, Yokohama, Japan). The Rho-kinase inhibitor Y27632 was provided by Mitsubishi Pharma.

Figure 6. **Cell spreading requires the interaction of talin with Tiam1 and integrin.** (A) Lysates of COS7 cells expressing Tiam1-C1199-HA were subjected to pull-down assay with GST-fused talin1 mutants. Tiam1 was barely detected in the eluates of beads containing talin1 A366/368. (B) GST-tagged integrin β3 cytoplasmic region (wild type or Y747A) was subjected to pull-down with lysates of COS7 cells expressing myc-talin1 (1–433 aa). Talin1 A366/368 bound to integrin β3, but talin1 A358 did not. (C) U251 cells transfected with talin1 siRNA and the indicated plasmids were stained with anti-GFP and anti-Tiam1 antibodies. Bars, 10 µm. Insets in the leftmost images (merged) are magnified in the panels to the right. The bar graph on the right represents the number of Tiam1-containing adhesions per 100 μm^2. Wild-type talin1 restored the inhibitory effect of talin1 knockdown on Tiam1, but the talin1 mutant A366/368 did not. (D) U251 cells transfected with the siRNA against talin1 and indicated plasmids were seeded onto FN under serum-free conditions. Rac1 activity was measured by pull-down with PAK-CRIB. Expression of wild-type talin1 rescued Rac1 activation, but that of the talin1 mutants failed to do so. Data represent the means ± SD of three independent experiments. (E) Transfected cells were seeded onto FN-coated dishes and immunostained 2 h later with anti-GFP antibody (green) and phalloidin (red). Bar, 10 µm. The bar graphs below represent quantifications of spread area and cell perimeter. *, $P < 0.05$; **, $P < 0.01$ versus respective control cells (Student's *t* test). Results are representative of more than three experiments.

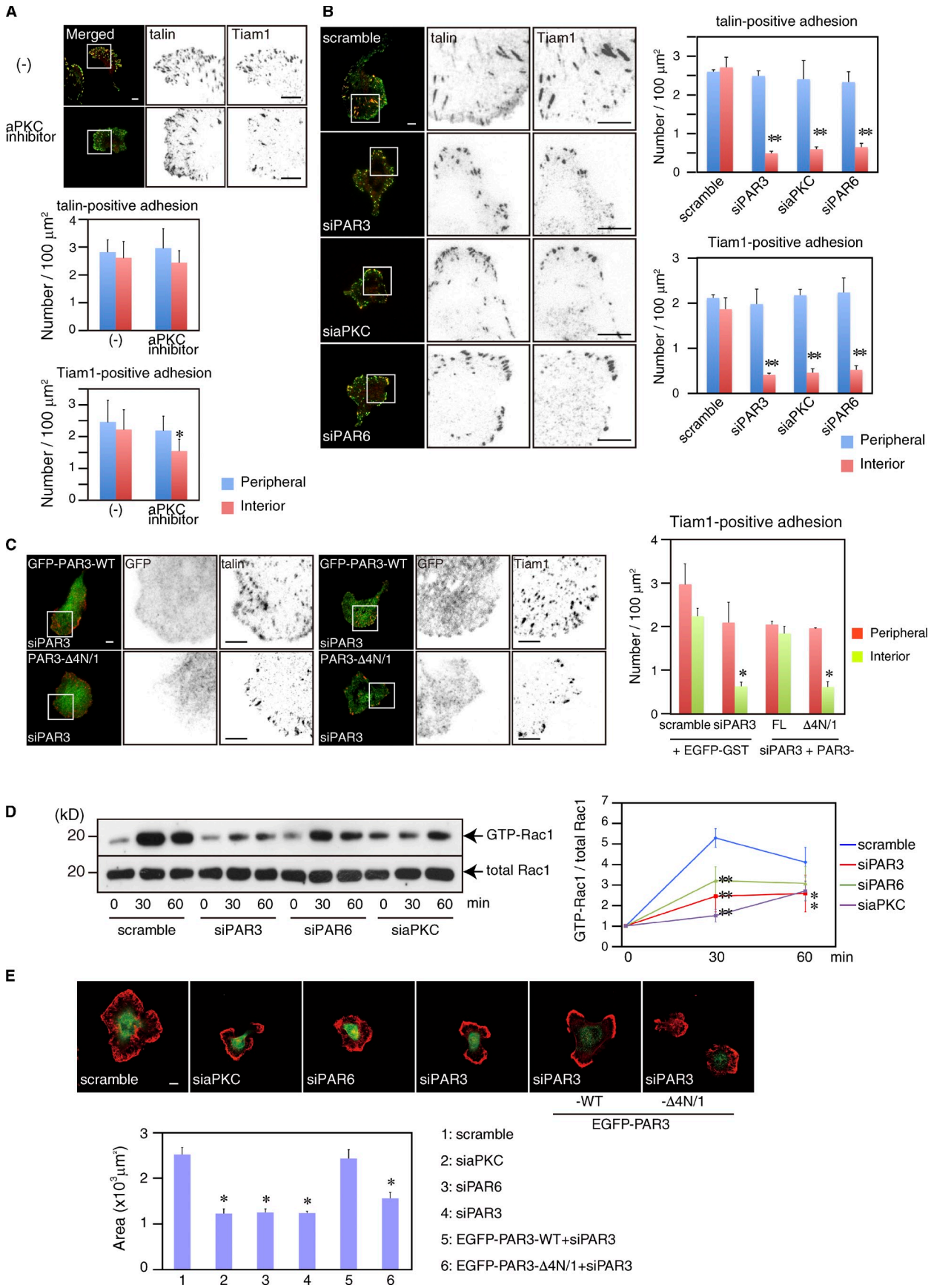

Cell culture and transfection

U251, COS7, Vero, HeLa, LN229, and HEK293 cells were maintained in DME (Sigma-Aldrich) supplemented with 10% fetal bovine serum (FBS; SAFC Biosciences). U251 and LN229 cells were transfected with Oligofectamine (Invitrogen) or with Amaxa Nucleofector (Lonza) according to the manufacturers' protocols. COS7, Vero, HeLa, and HEK293 cells were transfected with Lipofectamine2000 or Lipofectamine (Invitrogen) according to the manufacturer's protocol.

Protein purification and biochemistry

Recombinant proteins were produced in *Escherichia coli* (XL-1 Blue, BL21DE3, or RosettaDE3) with Isopropyl-β-D-thiogalactopyranoside and purified as described previously (Wang et al., 2007; Watanabe et al., 2009). In brief, the collected bacteria was suspended and subjected to the sonication. After the ultracentrifugation for 1 h at 100,000 *g*, the supernatants were applied to the column containing Glutathione Sepharose for GST fusions or Ni-NTA Sepharose for His fusions. After washing the columns, the proteins were eluted with the buffer containing reduced Glutathione or imidazole, and dialyzed against the appropriate buffer. All procedures of protein purification were performed at 4°C.

Affinity column chromatography, pull-down assay, and immunoprecipitation assay

Affinity column chromatography was performed as described previously (Kuroda et al., 1996; Fukata et al., 2002; Hikita et al., 2009). In brief, the cytosolic fraction of porcine brain homogenates was loaded onto Glutathione Sepharose 4B (GE Healthcare) coated with GST alone, GST-Tiam1-PHnCCEx, or GST-Tiam1-PDZ4. The columns were washed with buffer A (20 mM Tris/HCl, pH 8.0, 1 mM dithiothreitol, 1 mM EDTA, and protease inhibitors). Proteins bound to the affinity columns were eluted by buffer A containing 500 mM NaCl and identified as described elsewhere (Kuroda et al., 1996; Fukata et al., 2002). In brief, the eluates were electrophoresed and transferred onto a polyvinylidene difluoride membrane. The immobilized protein was reduced, S-carboxymethylated, and digested in situ with Achromobacter protease I (a Lys-C). Molecular mass analyses of Lys-C fragments were performed by matrix-assisted laser desorption/ionization time-of-flight mass spectrometry using a Voyager-DE/RP workstation (PerSeptive Biosystems). The proteins were identified by comparing the molecular weights determined with v/MS and theoretical peptide masses from the proteins registered in NCBI. For the pull-down assay, transfected COS7 cells were washed with PBS and lysed with Buffer B (20 mM Tris/HCl, pH 7.5, 1% Triton X-100, 50 mM NaCl, and protease inhibitors). After removing debris by centrifugation, the lysates were incubated with 1 nmol GST fusion proteins and Glutathione beads for 1 h at 4°C. The beads were washed with Buffer B and dissolved in SDS sample buffer. In the immunoprecipitation assay, appropriate antibodies and Protein A Sepharose (GE Healthcare) were used instead of GST fusion proteins and Glutathione beads. For endogenous association between talin and Tiam1, the lysates of U251 cells were cross-linked with 2% paraformaldehyde before immunoprecipitation as reported previously (Klockenbusch and Kast, 2010). The lysates were precipitated with anti-Tiam1 antibody and anti-Ras-GRF (Santa Cruz Biotechnology, Inc.) at 4 µg/ml.

Surface plasmon resonance-based binding assay

Direct binding was assessed using the BIAcore 3000 SPR system (GE Healthcare). GST-Tiam1-PDZ4 was immobilized to Sensor Chip CM5 with the amine coupling kit according to the manufacturer's protocol. His-talin (1–433 aa) was used as a ligand, and diluted in HBS-EP running buffer. Binding and kinetic analyses were performed using the BIAevaluation software.

In vitro binding assay of integrin with talin

To evaluate the binding of the talin mutants with integrin β3, we essentially followed methods described previously (Montanez et al., 2008). Glutathione beads coated with the indicated integrin β3 cytoplasmic region were incubated with lysates from COS7 cells expressing talin. The beads were washed with Buffer C (20 mM Tris/HCl, pH 7.0, 150 mM NaCl, 10 mM EDTA, 1% Triton X-100, 1 mM Na_3VO_4, and 50 mM NaF), and dissolved in SDS sample buffer.

Measuring active Rac1 by pull-down with PAK-CRIB

Cells were washed with chilled PBS and lysed with Buffer D (50 mM Tris/HCl, pH 7.5, 0.5% NP-40, 1 mM EGTA, 1 mM $MgCl_2$, 500 mM NaCl, and protease inhibitors) containing 0.5 mg/ml GST-PAK-CRIB. After removing debris by centrifugation, the lysates were incubated with Glutathione beads for 30 min at 4°C. The beads were washed with Buffer D and dissolved in SDS sample buffer. Aliquots of the lysate and eluates were immunoblotted with anti-Rac1 antibody to monitor total Rac1 and GTP-bound activated Rac1, respectively. For quantification, Rac1 activation (activated Rac1 / total Rac1) was normalized to that before seeding in each cell.

Immunohistochemical analysis

U251 cells were fixed with PBS containing 3.7% formaldehyde and 60% acetone for 20 min at −20°C, followed by permeabilization with 0.5% Triton X-100 for 20 min at RT. The cells were blocked with 1% BSA (Sigma-Aldrich) for 30 min at RT and incubated with primary for 1 h antibody at RT. For the experiments shown in Figs. 4 D, 6 E, and 7 E, the cells were fixed with 2% paraformaldehyde, and then permeabilized with 0.5% Triton X-100 for 10 min at RT. After washing with PBS, the cells were incubated with primary antibody for an additional 1 h at RT. To visualize talin and Tiam1, anti-talin (8d4), and anti-Tiam1 DHPH primary antibodies were used. The secondary antibodies were Alexa 488– and Alexa 555–conjugated antibodies against mouse IgG or rabbit IgG (Invitrogen). Conventional confocal images in a cell spreading assay were recorded by LSM5 pascal or LSM5 built around Axiovert 200M or 100M, respectively, under the control of LSM software (Carl Zeiss). TIRF images were taken with a microscope (model TE2000E; Nikon) using CFI Plan Apochromat TIRF X60 (NA 1.45) under the control of NIS-Elements equipped with an iXonEM+ 897 camera (Andor Technology) and a 488/561-nm excitation laser. We used the Dual band-pass dichroic (51004vs2bs; Chroma Technology Corp.), FF01-520/35 and FF01-593/40 (Semrock) as emission filters. For dynamic study of adhesions, the cells were observed at 37°C in HBSS supplemented with 10% FBS, 18 h after seeding on FN, with an inverted microscope (model IX-81; Olympus) using a Plan ApoN X60 oil objective (NA 1.42) under the control of MetaMorph software (Molecular Devices) equipped with an iXonEM+ DV885 camera (Andor Technology). We used a GFP filter set from Semrock (GFP-3035B). The images were processed by LSM software, NIS-Elements, or MetaMorph.

Quantification of micrographs and adhesion dynamics

Quantitative data were obtained using ImageJ (National Institutes of Health, Bethesda, MD). Cell area and perimeter were measured based on F-actin visualized by phalloidin staining. Quantification of protein colocalization was performed by first producing grayscale images of the appropriate channels and thresholding. Next, colocalization was determined using the plugin JACoP (Bolte and Cordelières, 2006). Cells were divided into two regions, the front region and the rest, by the following method: we defined the triangular region delineated by the center of the nucleus and both lateral edges of the protrusion based on immunofluorescence signals. Small adhesions were defined as those in which the area of talin immunofluorescence was greater than 0.6 μm^2 but less than 1.2 μm^2, and large adhesions as those greater than 1.2 μm^2, from a histogram showing the size distribution of adhesions in U251 cells (Fig. 3 B). Data analyses were

Figure 7. **The PAR complex is involved in Tiam1 targeting to adhesions and in signaling from integrin.** (A) Cells were treated with 40 µM aPKC inhibitor for 1 h before fixation and stained with talin (green) and Tiam1 (red) antibodies. The insets in the left panels are magnified in the right panels. Bars, 10 µm. (B) Cells transfected with the indicated siRNAs were stained with talin (green) and Tiam1 (red) antibodies. Bars, 10 µm. (C) Cells transfected with PAR3 siRNAs and the indicated plasmids were stained with GFP (green) and Tiam1 or talin (red) antibodies. Bars, 10 µm. Bar graphs below (A) or to the right (B and C) of the corresponding images represent the number of talin- or Tiam1-containing adhesions per 100 μm^2. (D) Adhesion-induced Rac1 activation in PAR complex–depleted cells. Depletion of the PAR complex attenuated Rac1 activation. The graph to the right quantifies Rac1 activation in these cells. Bars in the graph represent means ± SD. (E) Images of PAR complex–depleted cells at 2 h after spreading on FN. The cells were stained with anti-GFP antibody (green) and phalloidin (red). Bar, 10 µm. The bottom graph quantifies cell area after spreading. Data represent the means ± SD of at least three independent experiments. $n > 50$. *, $P < 0.05$; **, $P < 0.01$ versus respective control cells (A, B, and C, Tukey's HSD; D and E, Student's *t* test). Results are representative of more than three experiments.

performed using MS Excel. Statistical analyses (Student's *t* test or ANOVA/Tukey's post hoc test, as appropriate) were also done using Excel.

Adhesion dynamics were quantified as described previously (Franco et al., 2004; Webb et al., 2004). In brief, fluorescence intensities of individual EGFP-paxillin–inclusive adhesions from background-subtracted images were measured over time using MetaMorph. Changes (increase, assembly; decrease, disassembly) were plotted on separate semi-logarithmic graphs representing fluorescence intensity ratios over time. The slopes of linear regression trend lines fitted to the semi-logarithmic plots were then calculated to determine the apparent rate constants of assembly and the rate constant for disassembly. For each rate, measurements were made on at least 10 individual adhesions in 5 separate cells.

Boyden chamber assay

The migration index in the Boyden chamber assay was determined as described previously (Watanabe et al., 2009). siRNA was transfected into U251 cells with the indicated plasmid. Cell migration assays were performed using Transwell plates (pore size of 8 µm; HTS FluoroBlok Insert; BD). The undersurface of the membrane was coated for 1 h at RT with 10 µg/ml fibronectin (BD) diluted in distilled water. The cells were seeded in the upper chamber (10^4 per well) in 500 µl of DME with 0.1% BSA. DME supplemented with 0.1% BSA and 10% FBS was added to the lower chamber. The cells were allowed to migrate for 6 h. After fixation, both non-migrated and migrated EGFP-positive cells were counted by EGFP fluorescence, and the number of migrated cells was divided by total number of (migrated + non-migrated) cells. The value was expressed as a migration index. At least 300 EGFP-positive cells were counted in each group for each experiment.

Statistical analysis

Student's *t* test and analysis of variance (ANOVA) were performed after data were confirmed to fulfill the criteria of normal distribution and equal variance. If overall ANOVA was significant, we performed a post-hoc test. Tukey's honestly significant difference (HSD) multiple range test was performed.

Supplemental materials

Fig. S1 shows the characterization of our Tiam1 antibody and Tiam1 staining at adhesions. Fig. S2 represents the validation of siRNA and the relation between talins and Tiam1. Fig. S3 represents the involvement of Vav2 in adhesion-induced Rac1 activation in U251 cells. Fig. S4 shows the roles of a talin–Tiam1 complex in cell migration. Fig. S5 represents the participation of the PAR complex in Tiam1 targeting to adhesions and integrin outside-in signaling. Video 1 shows adhesion turnover in control cells. Videos 2 and 3 show adhesion turnover in talin- and Tiam1-depleted cells, respectively. Online supplemental material is available at http://www.jcb.org/cgi/content/full/jcb.201202041/DC1.

We thank I. Smith (Nara Institute of Science and Technology) for critical reading of the manuscript. We thank S. Ohno (Yokohama City University) for PAR3 cDNA, aPKC cDNA, and anti-PAR3 antibody; M. Inagaki (Aichi Cancer Center Research Institute) for U251 cells; R. Fässler (Max Planck Institute of Biochemistry) for GST-tagged integrin constructs; N. Kioka (Kyoto University) and S. Tadokoro (Osaka University) for sharing materials; D. Critchley and S. Monkley (University of Leicester) for anti-talin2 antibody; M. Matsuda (Kyoto University) for LN229 cells and RaichuEV-Rac; and all members of the Kaibuchi laboratory for discussion and support.

This work was supported by JST CREST (to K. Kaibuchi); KAKENHI (20227006 to K. Kaibuchi, 20790225 to T. Watanabe, and 23790247 to S. Wang); GCOE to K. Kaibuchi; and SCF to T. Watanabe.

Submitted: 8 February 2012
Accepted: 11 September 2012

References

Bolte, S., and F.P. Cordelières. 2006. A guided tour into subcellular colocalization analysis in light microscopy. *J. Microsc.* 224:213–232. http://dx.doi.org/10.1111/j.1365-2818.2006.01706.x

Bos, J.L., H. Rehmann, and A. Wittinghofer. 2007. GEFs and GAPs: critical elements in the control of small G proteins. *Cell*. 129:865–877. http://dx.doi.org/10.1016/j.cell.2007.05.018

Critchley, D.R. 2009. Biochemical and structural properties of the integrin-associated cytoskeletal protein talin. *Annu Rev Biophys*. 38:235–254. http://dx.doi.org/10.1146/annurev.biophys.050708.133744

del Pozo, M.A., L.S. Price, N.B. Alderson, X.D. Ren, and M.A. Schwartz. 2000. Adhesion to the extracellular matrix regulates the coupling of the small GTPase Rac to its effector PAK. *EMBO J.* 19:2008–2014. http://dx.doi.org/10.1093/emboj/19.9.2008

Etienne-Manneville, S. 2008. Polarity proteins in migration and invasion. *Oncogene*. 27:6970–6980. http://dx.doi.org/10.1038/onc.2008.347

Etienne-Manneville, S., and A. Hall. 2001. Integrin-mediated activation of Cdc42 controls cell polarity in migrating astrocytes through PKCzeta. *Cell*. 106:489–498. http://dx.doi.org/10.1016/S0092-8674(01)00471-8

Franco, S.J., M.A. Rodgers, B.J. Perrin, J. Han, D.A. Bennin, D.R. Critchley, and A. Huttenlocher. 2004. Calpain-mediated proteolysis of talin regulates adhesion dynamics. *Nat. Cell Biol.* 6:977–983. http://dx.doi.org/10.1038/ncb1175

Fukata, M., T. Watanabe, J. Noritake, M. Nakagawa, M. Yamaga, S. Kuroda, Y. Matsuura, A. Iwamatsu, F. Perez, and K. Kaibuchi. 2002. Rac1 and Cdc42 capture microtubules through IQGAP1 and CLIP-170. *Cell*. 109:873–885. http://dx.doi.org/10.1016/S0092-8674(02)00800-0

Fukata, M., M. Nakagawa, and K. Kaibuchi. 2003. Roles of Rho-family GTPases in cell polarisation and directional migration. *Curr. Opin. Cell Biol.* 15:590–597. http://dx.doi.org/10.1016/S0955-0674(03)00097-8

García-Mata, R., K. Wennerberg, W.T. Arthur, N.K. Noren, S.M. Ellerbroek, and K. Burridge. 2006. Analysis of activated GAPs and GEFs in cell lysates. *Methods Enzymol.* 406:425–437. http://dx.doi.org/10.1016/S0076-6879(06)06031-9

Garcia-Mata, R., E. Boulter, and K. Burridge. 2011. The 'invisible hand': regulation of RHO GTPases by RHOGDIs. *Nat. Rev. Mol. Cell Biol.* 12:493–504. http://dx.doi.org/10.1038/nrm3153

Goldstein, B., and I.G. Macara. 2007. The PAR proteins: fundamental players in animal cell polarization. *Dev. Cell*. 13:609–622. http://dx.doi.org/10.1016/j.devcel.2007.10.007

Guilluy, C., R. Garcia-Mata, and K. Burridge. 2011. Rho protein crosstalk: another social network? *Trends Cell Biol.* 21:718–726. http://dx.doi.org/10.1016/j.tcb.2011.08.002

Habets, G.G., E.H. Scholtes, D. Zuydgeest, R.A. van der Kammen, J.C. Stam, A. Berns, and J.G. Collard. 1994. Identification of an invasion-inducing gene, Tiam-1, that encodes a protein with homology to GDP-GTP exchangers for Rho-like proteins. *Cell*. 77:537–549. http://dx.doi.org/10.1016/0092-8674(94)90216-X

Hikita, T., S. Taya, Y. Fujino, S. Taneichi-Kuroda, K. Ohta, D. Tsuboi, T. Shinoda, K. Kuroda, Y. Funahashi, J. Uraguchi-Asaki, et al. 2009. Proteomic analysis reveals novel binding partners of dysbindin, a schizophrenia-related protein. *J. Neurochem.* 110:1567–1574. http://dx.doi.org/10.1111/j.1471-4159.2009.06257.x

Hillier, B.J., K.S. Christopherson, K.E. Prehoda, D.S. Bredt, and W.A. Lim. 1999. Unexpected modes of PDZ domain scaffolding revealed by structure of nNOS-syntrophin complex. *Science*. 284:812–815. http://dx.doi.org/10.1126/science.284.5415.812

Huttenlocher, A., and A.R. Horwitz. 2011. Integrins in cell migration. *Cold Spring Harb. Perspect. Biol.* 3:a005074. http://dx.doi.org/10.1101/cshperspect.a005074

Huveneers, S., and E.H. Danen. 2009. Adhesion signaling - crosstalk between integrins, Src and Rho. *J. Cell Sci.* 122:1059–1069. http://dx.doi.org/10.1242/jcs.039446

Hynes, R.O. 2002. Integrins: bidirectional, allosteric signaling machines. *Cell*. 110:673–687. http://dx.doi.org/10.1016/S0092-8674(02)00971-6

Iden, S., and J.G. Collard. 2008. Crosstalk between small GTPases and polarity proteins in cell polarization. *Nat. Rev. Mol. Cell Biol.* 9:846–859. http://dx.doi.org/10.1038/nrm2521

Itoh, R.E., K. Kurokawa, Y. Ohba, H. Yoshizaki, N. Mochizuki, and M. Matsuda. 2002. Activation of rac and cdc42 video imaged by fluorescent resonance energy transfer-based single-molecule probes in the membrane of living cells. *Mol. Cell. Biol.* 22:6582–6591. http://dx.doi.org/10.1128/MCB.22.18.6582-6591.2002

Itoh, N., M. Nakayama, T. Nishimura, S. Fujisue, T. Nishioka, T. Watanabe, and K. Kaibuchi. 2010. Identification of focal adhesion kinase (FAK) and phosphatidylinositol 3-kinase (PI3-kinase) as Par3 partners by proteomic analysis. *Cytoskeleton (Hoboken)*. 67:297–308.

Jaffe, A.B., and A. Hall. 2005. Rho GTPases: biochemistry and biology. *Annu. Rev. Cell Dev. Biol.* 21:247–269. http://dx.doi.org/10.1146/annurev.cellbio.21.020604.150721

Jarzynka, M.J., B. Hu, K.M. Hui, I. Bar-Joseph, W. Gu, T. Hirose, L.B. Haney, K.S. Ravichandran, R. Nishikawa, and S.Y. Cheng. 2007. ELMO1 and Dock180, a bipartite Rac1 guanine nucleotide exchange factor, promote human glioma cell invasion. *Cancer Res.* 67:7203–7211. http://dx.doi.org/10.1158/0008-5472.CAN-07-0473

Kawano, Y., Y. Fukata, N. Oshiro, M. Amano, T. Nakamura, M. Ito, F. Matsumura, M. Inagaki, and K. Kaibuchi. 1999. Phosphorylation of

myosin-binding subunit (MBS) of myosin phosphatase by Rho-kinase in vivo. *J. Cell Biol.* 147:1023–1038. http://dx.doi.org/10.1083/jcb.147.5.1023

Kawataki, T., T. Yamane, H. Naganuma, P. Rousselle, I. Andurén, K. Tryggvason, and M. Patarroyo. 2007. Laminin isoforms and their integrin receptors in glioma cell migration and invasiveness: Evidence for a role of alpha5-laminin(s) and alpha3beta1 integrin. *Exp. Cell Res.* 313:3819–3831. http://dx.doi.org/10.1016/j.yexcr.2007.07.038

Kim, C., F. Ye, and M.H. Ginsberg. 2011. Regulation of integrin activation. *Annu. Rev. Cell Dev. Biol*. 27:321–345. http://dx.doi.org/10.1146/annurev-cellbio-100109-104104

Klockenbusch, C., and J. Kast. 2010. Optimization of formaldehyde cross-linking for protein interaction analysis of non-tagged integrin beta1. *J. Biomed. Biotechnol.* 2010:927585. http://dx.doi.org/10.1155/2010/927585

Kraynov, V.S., C. Chamberlain, G.M. Bokoch, M.A. Schwartz, S. Slabaugh, and K.M. Hahn. 2000. Localized Rac activation dynamics visualized in living cells. *Science*. 290:333–337. http://dx.doi.org/10.1126/science.290.5490.333

Kuroda, S., M. Fukata, K. Kobayashi, M. Nakafuku, N. Nomura, A. Iwamatsu, and K. Kaibuchi. 1996. Identification of IQGAP as a putative target for the small GTPases, Cdc42 and Rac1. *J. Biol. Chem.* 271:23363–23367. http://dx.doi.org/10.1074/jbc.271.38.23363

Machacek, M., L. Hodgson, C. Welch, H. Elliott, O. Pertz, P. Nalbant, A. Abell, G.L. Johnson, K.M. Hahn, and G. Danuser. 2009. Coordination of Rho GTPase activities during cell protrusion. *Nature*. 461:99–103. http://dx.doi.org/10.1038/nature08242

Montanez, E., S. Ussar, M. Schifferer, M. Bösl, R. Zent, M. Moser, and R. Fässler. 2008. Kindlin-2 controls bidirectional signaling of integrins. *Genes Dev.* 22:1325–1330. http://dx.doi.org/10.1101/gad.469408

Moser, M., K.R. Legate, R. Zent, and R. Fässler. 2009. The tail of integrins, talin, and kindlins. *Science*. 324:895–899. http://dx.doi.org/10.1126/science.1163865

Nakayama, M., T.M. Goto, M. Sugimoto, T. Nishimura, T. Shinagawa, S. Ohno, M. Amano, and K. Kaibuchi. 2008. Rho-kinase phosphorylates PAR-3 and disrupts PAR complex formation. *Dev. Cell*. 14:205–215. http://dx.doi.org/10.1016/j.devcel.2007.11.021

Nayal, A., D.J. Webb, C.M. Brown, E.M. Schaefer, M. Vicente-Manzanares, and A.R. Horwitz. 2006. Paxillin phosphorylation at Ser273 localizes a GIT1-PIX-PAK complex and regulates adhesion and protrusion dynamics. *J. Cell Biol.* 173:587–589. http://dx.doi.org/10.1083/jcb.200509075

Nishimura, T., and K. Kaibuchi. 2007. Numb controls integrin endocytosis for directional cell migration with aPKC and PAR-3. *Dev. Cell*. 13:15–28. http://dx.doi.org/10.1016/j.devcel.2007.05.003

Nishimura, T., T. Yamaguchi, K. Kato, M. Yoshizawa, Y.-i. Nabeshima, S. Ohno, M. Hoshino, and K. Kaibuchi. 2005. PAR-6-PAR-3 mediates Cdc42-induced Rac activation through the Rac GEFs STEF/Tiam1. *Nat. Cell Biol.* 7:270–277. http://dx.doi.org/10.1038/ncb1227

Parsons, J.T., A.R. Horwitz, and M.A. Schwartz. 2010. Cell adhesion: integrating cytoskeletal dynamics and cellular tension. *Nat. Rev. Mol. Cell Biol.* 11:633–643. http://dx.doi.org/10.1038/nrm2957

Pegtel, D.M., S.I.J. Ellenbroek, A.E.E. Mertens, R.A. van der Kammen, J. de Rooij, and J.G. Collard. 2007. The Par-Tiam1 complex controls persistent migration by stabilizing microtubule-dependent front-rear polarity. *Curr. Biol.* 17:1623–1634. http://dx.doi.org/10.1016/j.cub.2007.08.035

Pertz, O., L. Hodgson, R.L. Klemke, and K.M. Hahn. 2006. Spatiotemporal dynamics of RhoA activity in migrating cells. *Nature*. 440:1069–1072. http://dx.doi.org/10.1038/nature04665

Petrie, R.J., A.D. Doyle, and K.M. Yamada. 2009. Random versus directionally persistent cell migration. *Nat. Rev. Mol. Cell Biol.* 10:538–549. http://dx.doi.org/10.1038/nrm2729

Price, L.S., J. Leng, M.A. Schwartz, and G.M. Bokoch. 1998. Activation of Rac and Cdc42 by integrins mediates cell spreading. *Mol. Biol. Cell*. 9:1863–1871.

Ridley, A.J., M.A. Schwartz, K. Burridge, R.A. Firtel, M.H. Ginsberg, G. Borisy, J.T. Parsons, and A.R. Horwitz. 2003. Cell migration: integrating signals from front to back. *Science*. 302:1704–1709. http://dx.doi.org/10.1126/science.1092053

Rooney, C., G. White, A. Nazgiewicz, S.A. Woodcock, K.I. Anderson, C. Ballestrem, and A. Malliri. 2010. The Rac activator STEF (Tiam2) regulates cell migration by microtubule-mediated focal adhesion disassembly. *EMBO Rep.* 11:292–298. http://dx.doi.org/10.1038/embor.2010.10

Rossman, K.L., C.J. Der, and J. Sondek. 2005. GEF means go: turning on RHO GTPases with guanine nucleotide-exchange factors. *Nat. Rev. Mol. Cell Biol.* 6:167–180. http://dx.doi.org/10.1038/nrm1587

Suzuki, A., and S. Ohno. 2006. The PAR-aPKC system: lessons in polarity. *J. Cell Sci.* 119:979–987. http://dx.doi.org/10.1242/jcs.02898

ten Klooster, J.P., Z.M. Jaffer, J. Chernoff, and P.L. Hordijk. 2006. Targeting and activation of Rac1 are mediated by the exchange factor beta-Pix. *J. Cell Biol.* 172:759–769. http://dx.doi.org/10.1083/jcb.200509096

Wang, S., T. Watanabe, J. Noritake, M. Fukata, T. Yoshimura, N. Itoh, T. Harada, M. Nakagawa, Y. Matsuura, N. Arimura, and K. Kaibuchi. 2007. IQGAP3, a novel effector of Rac1 and Cdc42, regulates neurite outgrowth. *J. Cell Sci.* 120:567–577. http://dx.doi.org/10.1242/jcs.03356

Watanabe, T., J. Noritake, M. Kakeno, T. Matsui, T. Harada, S. Wang, N. Itoh, K. Sato, K. Matsuzawa, A. Iwamatsu, et al. 2009. Phosphorylation of CLASP2 by GSK-3beta regulates its interaction with IQGAP1, EB1 and microtubules. *J. Cell Sci.* 122:2969–2979. http://dx.doi.org/10.1242/jcs.046649

Webb, D.J., K. Donais, L.A. Whitmore, S.M. Thomas, C.E. Turner, J.T. Parsons, and A.F. Horwitz. 2004. FAK-Src signalling through paxillin, ERK and MLCK regulates adhesion disassembly. *Nat. Cell Biol.* 6:154–161. http://dx.doi.org/10.1038/ncb1094

Xia, N., C.K. Thodeti, T.P. Hunt, Q. Xu, M. Ho, G.M. Whitesides, R. Westervelt, and D.E. Ingber. 2008. Directional control of cell motility through focal adhesion positioning and spatial control of Rac activation. *FASEB J.* 22:1649–1659. http://dx.doi.org/10.1096/fj.07-090571

Zaidel-Bar, R., S. Itzkovitz, A. Ma'ayan, R. Iyengar, and B. Geiger. 2007. Functional atlas of the integrin adhesome. *Nat. Cell Biol.* 9:858–867. http://dx.doi.org/10.1038/ncb0807-858

Zhang, X., G. Jiang, Y. Cai, S.J. Monkley, D.R. Critchley, and M.P. Sheetz. 2008. Talin depletion reveals independence of initial cell spreading from integrin activation and traction. *Nat. Cell Biol.* 10:1062–1068. http://dx.doi.org/10.1038/ncb1765